Supporting Information

Enhanced green Light-harvesting and PS II-Loading in CdTe QDs embedded IO-SnO_2 bio-photoanodes for photocurrent generation

Zaigui Yuan [a, †], Jiakang Li [a, †], Xiyun Feng [a,*], Ting Ma [a], Liangfei Duan [a], Jun Wang [a] , Xufeng Zhang [a], Yi Jia [b,*] Jiao Li [c,*] and Jing Shen [a,*]

---

[a] *Yunnan Key Laboratory of Modern Separation Analysis and Substance Transformation, College of Chemistry and Chemical Engineering, Yunnan Normal University, Kunming, 650500, Yunnan, PR China*

[b] *Beijing National Laboratory for Molecular Sciences (BNLMS), CAS Key Lab of Colloid, Interface and Chemical Thermodynamics, Institute of Chemistry, Chinese Academy of Science, Beijing 100190, China*

[c] *School of Materials Science and Engineering, Shijiazhuang Tiedao University, Shijiazhuang, Hebei,050043, PR China*

* *Corresponding author* ***E-mail address****: XiyunFeng@yunu.edu.cn (X.Y. Feng), jiayi@iccas.ac.cn (Y.Jia),taixiella@163.com (J.Li), shenjing@ynnu.edu.cn(J.Shen)*

---

† These authors share equal contribution to this work.

Text S1 Chemical

Styrene (99%), Ethanol absolute (EtOH, ≥ 99.7%), Potassium persulfate ($K_2S_2O_8$, ≥ 99.5%), Sodium hydroxide pellets (NaOH, 96%), Triton X-100 (Mw: average 625), Poly (ethyleneimine) solution (PEI, 50 wt.% , Mw-750000), Sodium sulfate pentahydrate (Na_2SO_4, 99.0%), Tin (IV) chloride pentahydrate ($SnCl_4$·$5H_2O$, 99.0%), Titanium dioxide (P25, 20nm, 99.8%), Tricine (99%), BSA (≥ 98%), Magnesium chloride ($MgCl_2$, 99%), C-Ascorrbic acid (Vc, 99.0%), Sucrose, MES (≥ 99%), Betaine (98%), Calcium chloride ($CaCl_2$, 96.0%), Sodium chloride (NaCl, ≥ 99.5%), Acetone (CH_3COCH_3, ≥ 99.5%), Poly (allylamine hydrochloride) (PAH, 98%), 3-Mercaptopropionic acid ($C_3H_6O_2S$, 98%), Sodium tellurite (Na_2TeO_3, 99.9%), 2,5-Dichloro-1,4-benzoquinone (DCBQ, ≥ 98%), Sodium Tetrahydroborate ($NaBH_4$, ≥ 98.0%), Caclmium chloride hemi(pentahydrate) ($CdCl_2$•$5H_2O$, 99.95%), Diuron (99.5%), 2,6-Dichlorophenolindophenol (97%), All the chemicals used in this work were of analytical grade received from Macklin.

Text S2 Characterization

The morphology of various CdTe quantum dots (QDs) and the working electrode was characterized using transmission electron microscopy (TEM) with a JEM-2100F field emission electron microscope (JEOL Ltd., Tokyo, Japan). The composition and chemical structure were analyzed via Fourier transform infrared (FT-IR) spectroscopy employing a Nicolet Is5 spectrometer (Thermo Fisher Scientific, Waltham, MA, USA). X-ray photoelectron spectroscopy (XPS) analysis was conducted using a Thermo Scientific K-Alpha photoelectron spectrometer (USA). The XPS analysis utilized an Al Kα X-ray source (hν = 1486.6 eV) under the following conditions: a spot size of 400 μm, chamber pressure maintained below 5×10^{-7} mbar, an operating voltage of 12 kV, a filament current of 6 mA, an electron emission angle of 60°, and an instrument work function of 4.2 eV. Binding energies were calibrated using the C1s peak at 284.80 eV as a reference for charge correction. Raman spectra were recorded with a LabRAM HR Evolution (Horiba Ltd., Kyoto, Japan). UV–vis absorption spectra were obtained using a TU-1901 double beam UV–vis spectrophotometer (Persee General Instrument Ltd., Beijing, China). The photoluminescence properties of the different CdTe QDs were assessed using an FLS1000 spectrofluorometer (Edinburgh Instruments, Livingston, UK). The zeta potential of the CdTe QDs and IO-SnO_2 was measured to evaluate their potential.

Text S3 the synthetic of the Polystyrene spheres

Polystyrene microspheres were synthesized using established methods reported in the literature[1] [2] [3]. Impurities that inhibit the polymerization reaction were removed by washing the styrene three times with 2 M NaOH, followed by neutralization with deionized water. Under a nitrogen atmosphere, 86 mL of deionized water was heated to 72 ° C in an oil bath. Subsequently, 4 mL of pre-treated styrene was added to the system. After thorough mixing via mechanical stirring, 10 mL of $K_2S_2O_8$ (0.12 g) was introduced as the initiator for the polymerization reaction. The reaction was allowed to proceed for 12 hours before termination. The polystyrene microspheres were collected after the mixture cooled to room temperature. The resulting microspheres were thoroughly washed through repeated centrifugation, decantation, and re-dispersion in ethanol and deionized water three times to ensure complete purification.

Text S4 the fabrication of the IO-SnO_2

IO-SnO_2 was prepared according to the method reported previously. [2,3,4] The conductive glass (1 cm × 4 cm) was meticulously cleaned using deionized water, followed by ethanol. A dispersion of polystyrene (PS) spheres, with a diameter of 500 nm and a concentration of approximately 0.3 wt % (4 mL), was introduced into a glass bottle, which was subsequently sealed with a piece of parafilm featuring a slit. The cleaned indium tin oxide (ITO) glass slide was inserted through the slit and positioned against the side of the glass bottle. The bottle was then placed in an oven at 50 °C for a duration of 20 to 25 hours. Following this, the PS film was gradually immersed in the tin oxide (SnO_2) precursor solution for 30 seconds. This solution was prepared by dissolving 1.05 g of $SnCl_4 \cdot 5H_2O$ in 30 mL of a deionized water and ethanol mixture (1:1). After allowing the film to dry naturally, the immersion process was repeated twice. The resulting opal film was subsequently transferred to a muffle furnace, where it was annealed from room temperature to 500 °C at a heating rate of 1 °C/min and maintained at 500 °C for 4 hours to obtain IO-SnO_2.

Text S5 the generation of the CdTe QDs

228 mg of $CdCl_2 \bullet 5H_2O$ was dissolved in 50 mL of deionized water, and 148 μL of MPA was added. The pH was adjusted to 10.5 using 2 M NaOH. Under a nitrogen

atmosphere, 22 mg of Na_2TeO_3 was dissolved in 50 mL of deionized water and added to the above solution. After stirring for 10 minutes, 200 mg of $NaBH_4$ was added to the solution. The mixture was refluxed at 100 °C in an oil bath for 3 hours to obtain the desired CdTe quantum dots[5].

Text S6 the LBL self-assembly of the composite electrode

The PAH/CdTe multilayer film was assembled on IO-SnO_2 using the layer-by-layer assembly technique. The IO-SnO_2 was immersed in a PAH solution (0.2 mg•mL^{-1}, 0.3 M NaCl) for 15 minutes, followed by three washes with deionized water for 3 minutes, 1 minute and 1 minute, respectively. It was then immersed in a CdTe QDs solution (110 mM) for 15 minutes, followed by three more washes with deionized water for 3 minutes, 1 minute and 1 minute, respectively. The above process was repeated to obtain a multilayer film of PAH/CdTe QDs.

Text S7 Isolation of PS II enzyme.

Photosystem II was extracted according to our previously reported method[6] [7]. Spinach was purchased from the market. After washing, 200 g of leaves were stored in the dark at 4 ℃ overnight. The spinach was then placed into a pre-cooled juicer, mixed with 200 mL of buffer B1 (0.4 M sucrose, 20 mM Tricine ± NaOH pH 7.8, 2 mM $MgCl_2$, 40 mM NaCl, 2 mM Vc, 0.2% BSA), and ground. The mixture was subsequently filtered through cheesecloth. The filtrate was centrifuged at 200 g for 2 minutes, and the supernatant was collected. The supernatant was then centrifuged at 1000 g for 15 minutes to obtain the pellet, which was resuspended in a hypotonic buffer B2 (20 mM Tricine ± NaOH pH 7.8, 5 mM $MgCl_2$, 10 Mm NaCl, 0.2% BSA) and stirred for 15 minutes. This centrifugation process was repeated. The resulting pellet was resuspended in buffer B3 (0.4 M sucrose, 20 mM MES ± NaOH pH 6.5, 15 Mm NaCl, 5m M $MgCl_2$) to obtain purified thylakoid membranes. The chloroplast concentration was quantified according to equation (1), and the concentration was adjusted to 2.5 mg•mL^{-1} by adding buffer B3. The thylakoid membranes were then resuspended in buffer B4 (0.4 M sucrose, 20 mM MES ± NaOH pH 6.5, 15 Mm NaCl, 5 mM $MgCl_2$, 20% TX-100) with Triton-X 100 at a ratio of Triton-X 100 to chloroplasts (w:w=20:1). The mixture was centrifuged at 10000 g for 1 minute to collect the supernatant, which was then centrifuged again at 24000 g for 15 minutes. The final pellet obtained was the thylakoid membrane enriched in PSII, and the protein concentration was determined according to equation (1).

$$[chl] = \{8.02 \times (A663 - A720) + 20.21 \times (A645 - A720)\} \times dicution\ fictor \tag{1}$$

Text S8 Electrochemical measurements

An electrochemical workstation (CHI660E, Shanghai, CH. Instruments, China) with a standard three electrode model was employed to conduct photocurrent response measurements. The working electrodes used were the ITO conductive glass and the prepared electrodes. The Ag/ AgCl electrode and platinum wire were utilized as the reference and the counter electrode, respectively. 0.1 M Na_2SO_4 solution was employed as the electrolyte. A 300 W Xenon lamp with a 420 nm cutoff filter was used as the external light source.

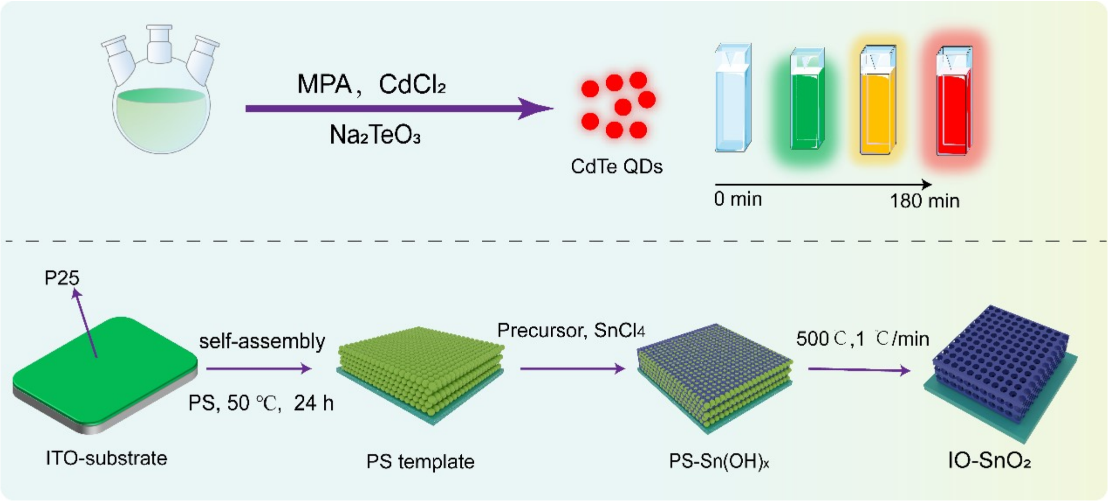

Fig S1. Schematic diagram of quantum dot and IO-SnO_2 electrode fabrication.

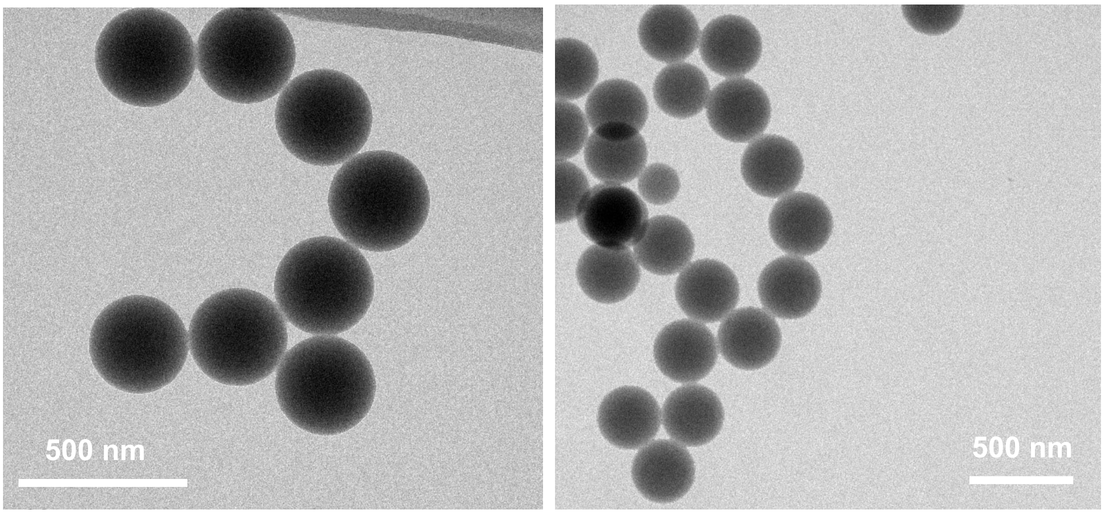

Fig.S2 the TEM image of the Polystyrene.

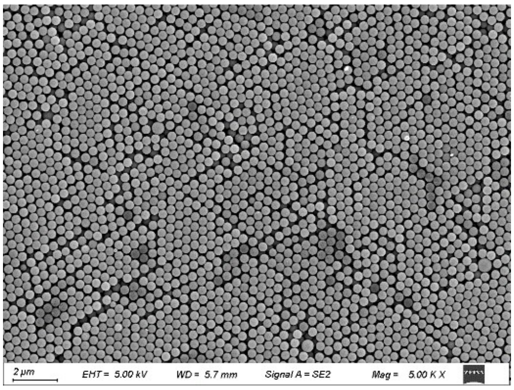

Fig.S3 the SEM image of the Polystyrene arrays template.

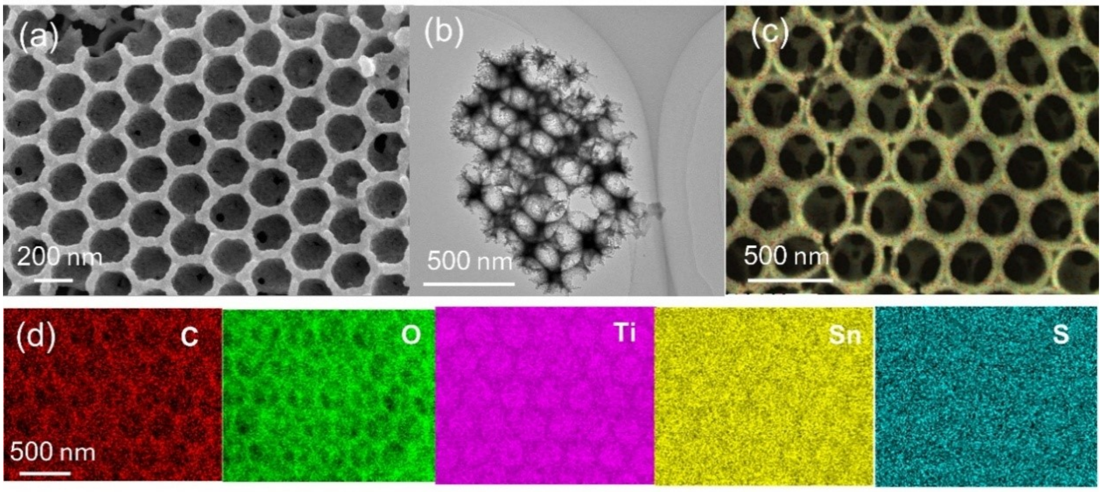

Fig.S4 the SEM, TEM image of the IO-SnO_2. (a) SEM images of IO-SnO_2, (b) TEM images of IO-SnO_2, (c) The area selected for EDS analysis, (d) EDS analysis.

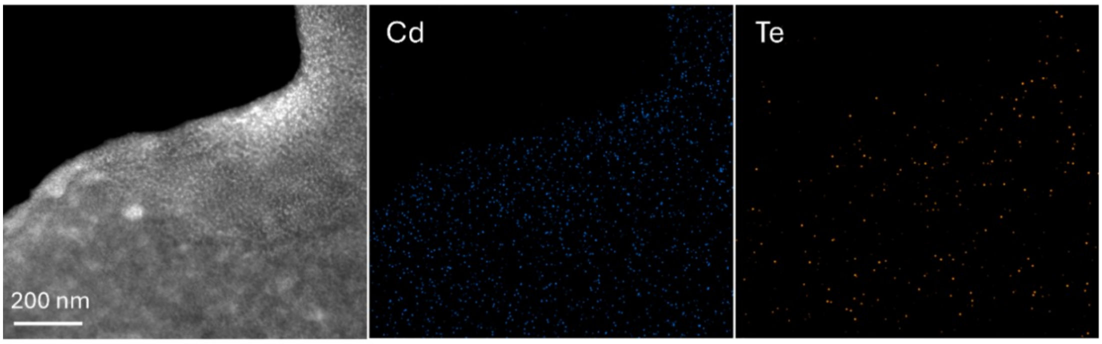

Fig.S5 the TEM image of the CdTe QDs and the distribution of the element mapping.

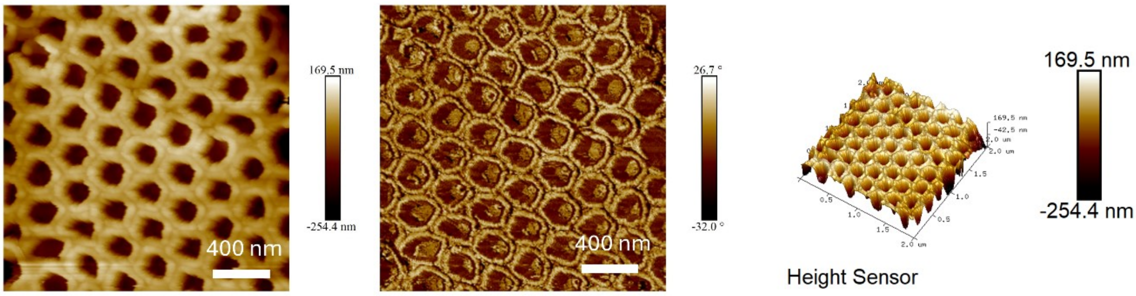

Fig.S6 the AFM image of IO-SnO_2 electrode

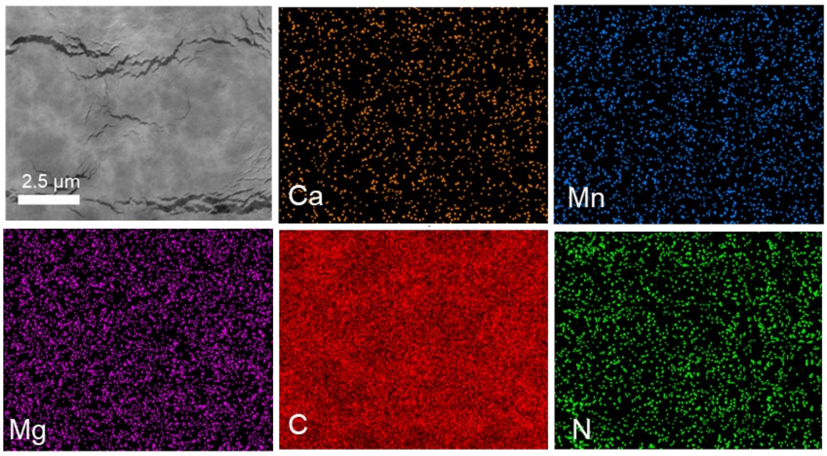

Fig.S7 the SEM image of the PS II enzyme and the element EDS mapping of Ca, Mn, Mg, C and N.

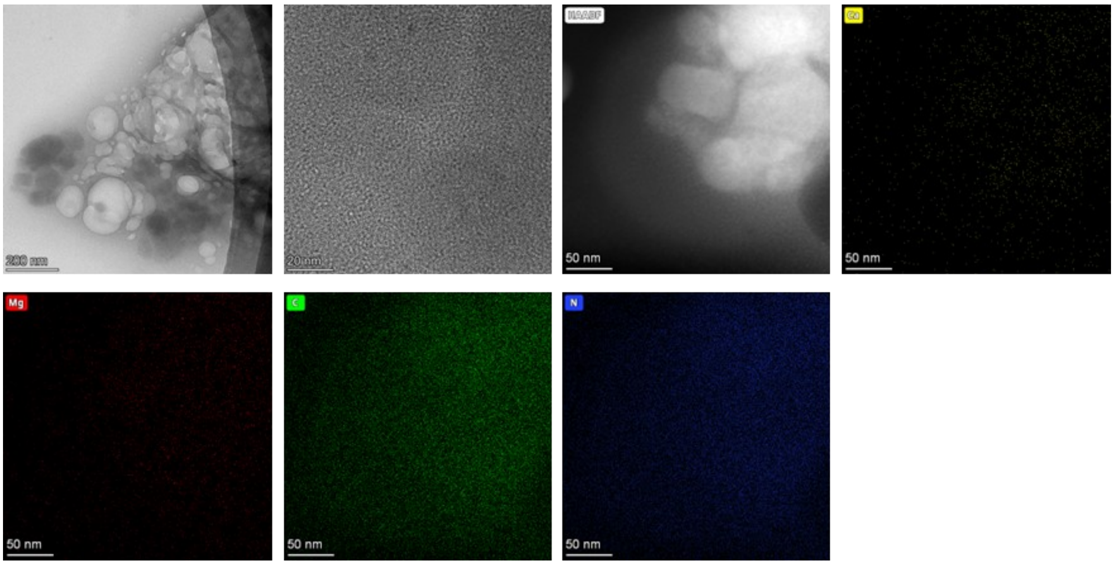

Fig.S8 the TEM image and the element EDS mapping of the PS II enzyme including Ca, Mg, C and N.

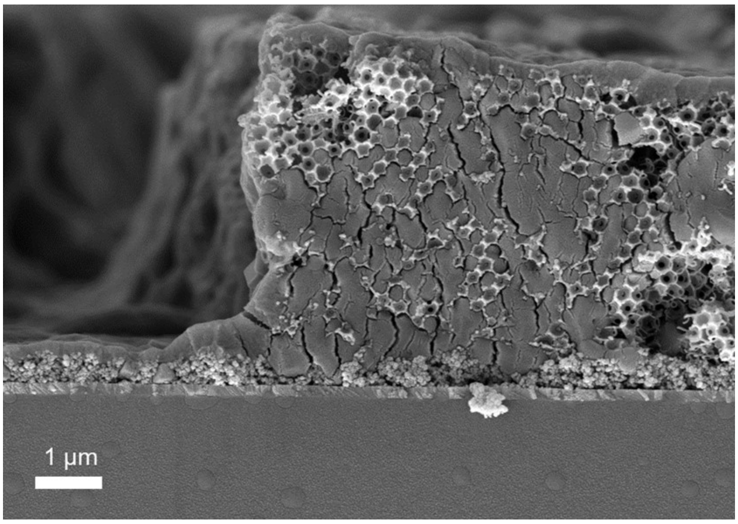

Fig.S9 the SEM image of the IO-SnO_2/CdTe QDs/PS II electrode

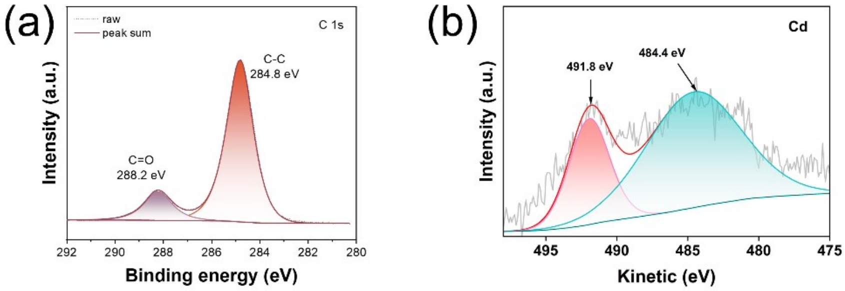

Fig.S10 XPS analysis of CdTe quantum dots. (a) represents the C $_{1s}$ spectrum, (b) Auger spectrum of Cd and

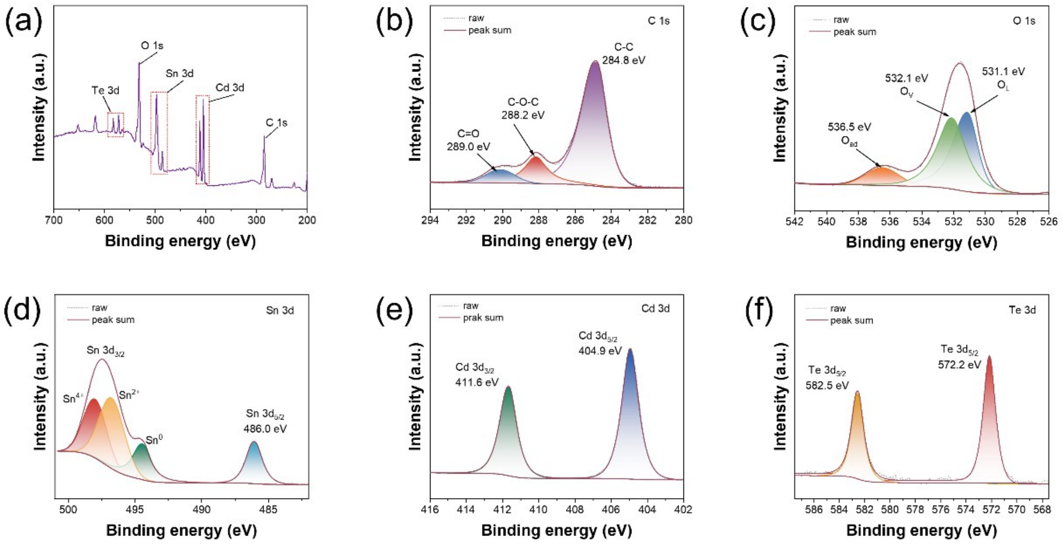

Fig.S11 XPS analysis of the composite electrode. (a) The XPS full spectrum scan of the composite electrode (b) represents the C 1s spectrum, (c) represents the O 1s spectrum (d) represents the Sn 3d spectrum, (e) represents the Cd 3d spectrum. (f) represents the Te 3d spectrum,

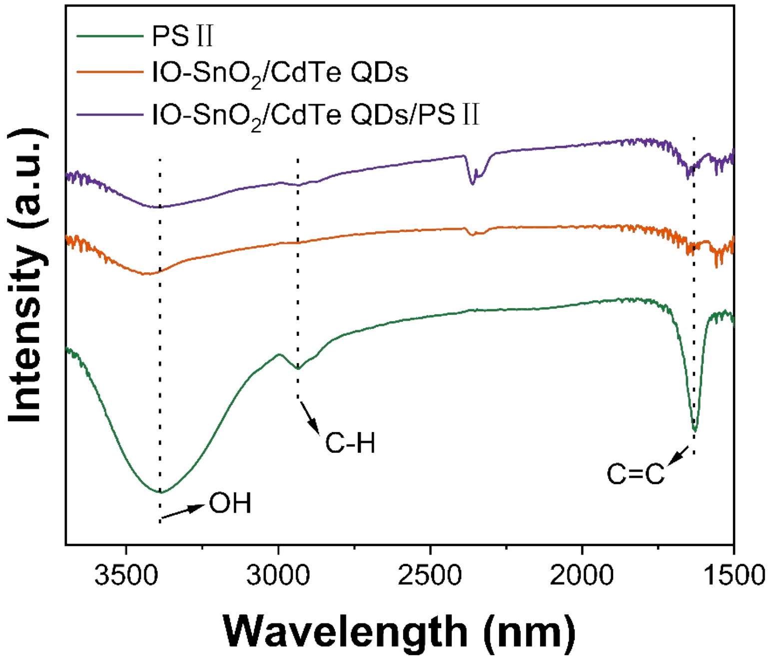

Fig.S12 The FT-IR image pf the IO-SnO_2 electrode, CdTe QDs and PS II.

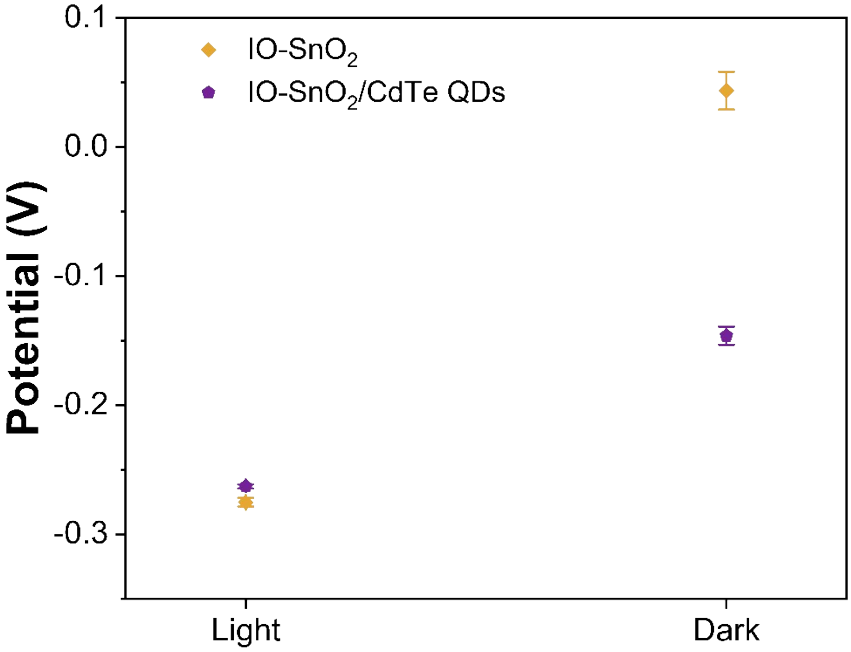

Fig.S13 Open-circuit voltage of electrodes IO-SnO_2 and IO-SnO_2 /CdTe QDs.

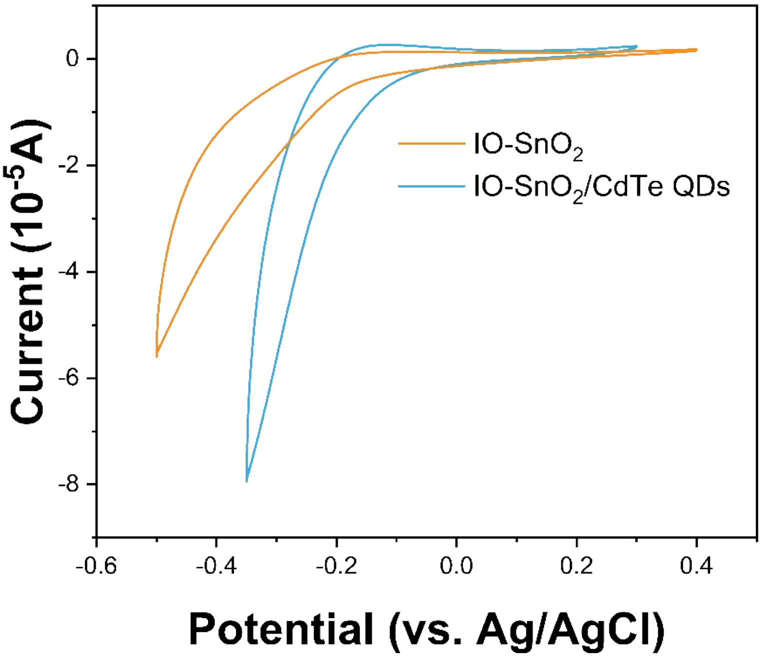

Fig.S14 Cyclic voltammetry tests of electrodes IO-SnO_2 and IO-SnO_2 /CdTe QDs.

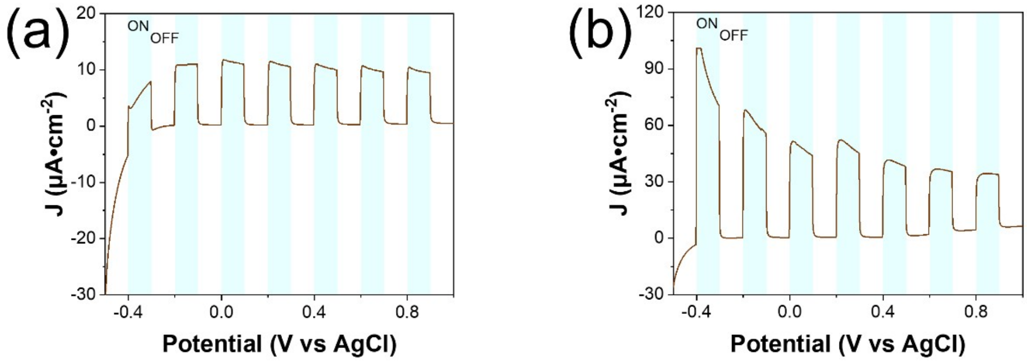

Fig.S15 Linear sweep voltammetry tests of electrodes (a) IO-SnO_2 and (b) IO-SnO_2 /CdTe QDs.

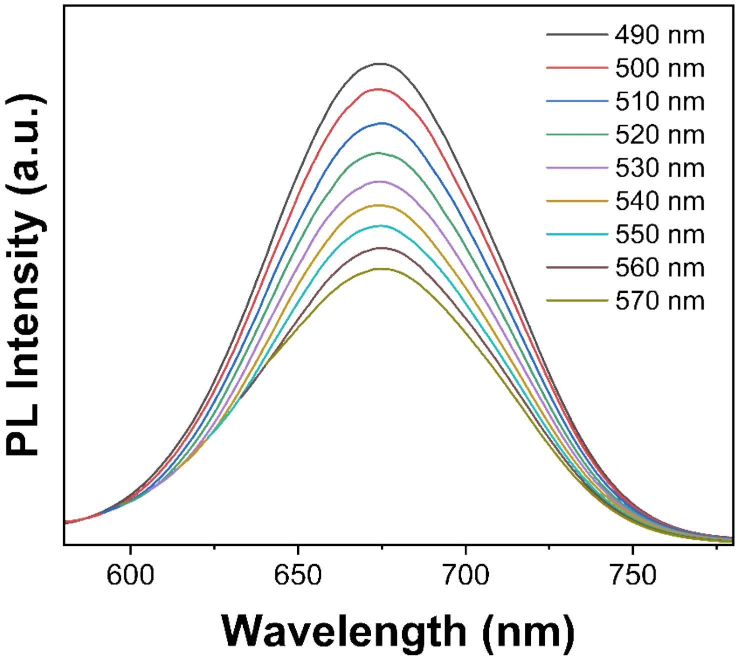

Fig.S16 Fluorescence measurements of 27.5 mM quantum dots at different excitation wavelengths within the green light range.

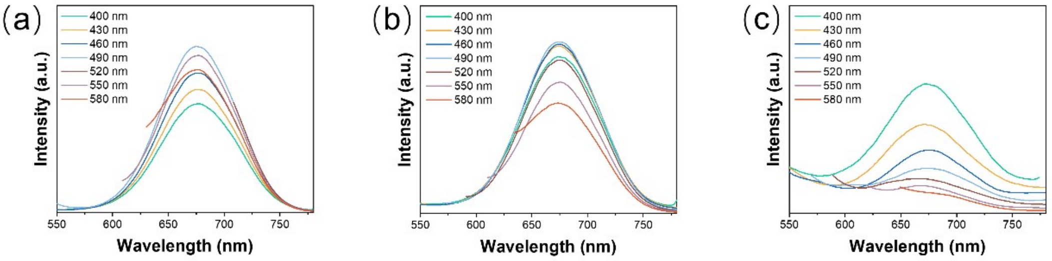

Fig.S17 Fluorescence measurements of quantum dots at different excitation wavelengths and concentrations. (a)110 mM CdTe QDs (b) 55 mM CdTe QDs (c) 1.1 mM CdTe QDs.

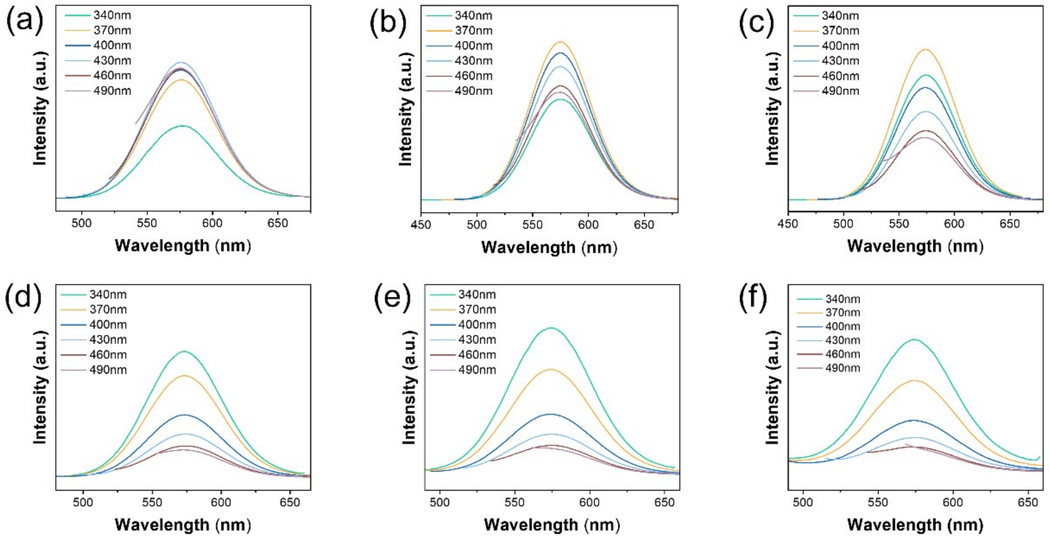

Fig.S18 The fluorescence measurements of CdTe QDs with an emission peak center at 580 nm were conducted at different excitation wavelengths for various concentrations. The concentrations tested were (a) 110 mM, (b) 55 mM, (c) 27.5 mM, (d) 11 mM, (e) 5.5 mM, and (f) 1.1 mM.

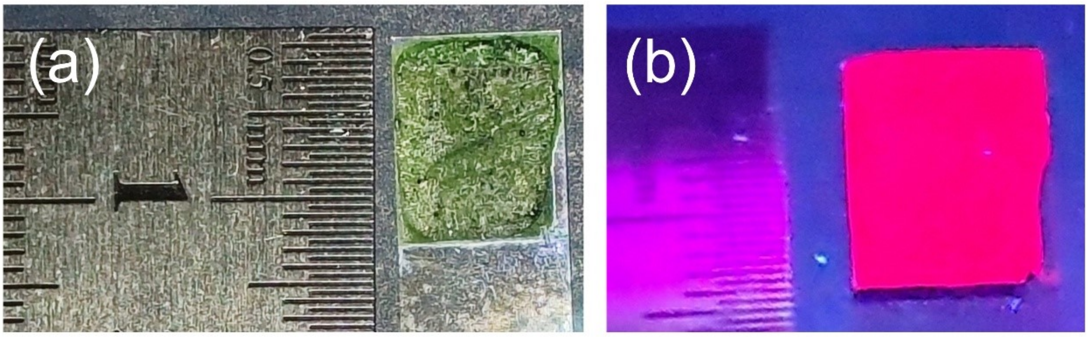

Fig.S19 Photographs of IO-SnO_2/CdTe QDs/PSII under visible light and fluorescence illumination. (a) IO-SnO_2/CdTe QDs/PSII electrode under natural light, (b) IO-SnO_2/CdTe QDs/PSII electrode under 365 nm light.

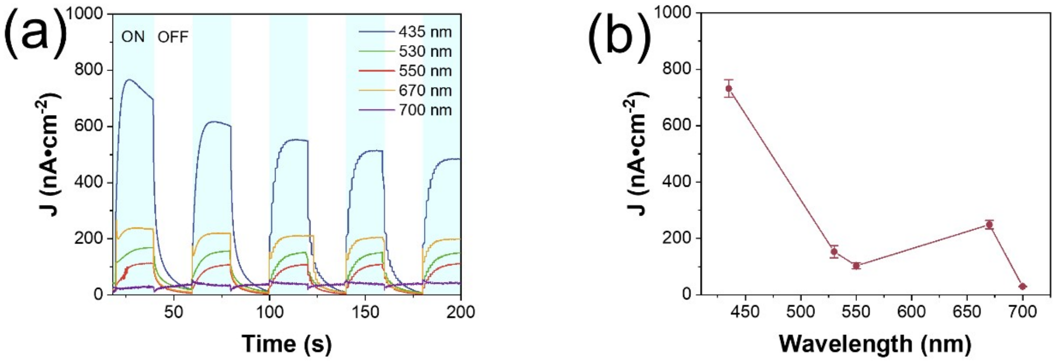

Fig.S20 Photocurrent measurements of IO-SnO_2/PSII under different wavelengths, with error bar analysis: (a) Photocurrent corresponding to different wavelengths, (b) Error analysis under different wavelengths.

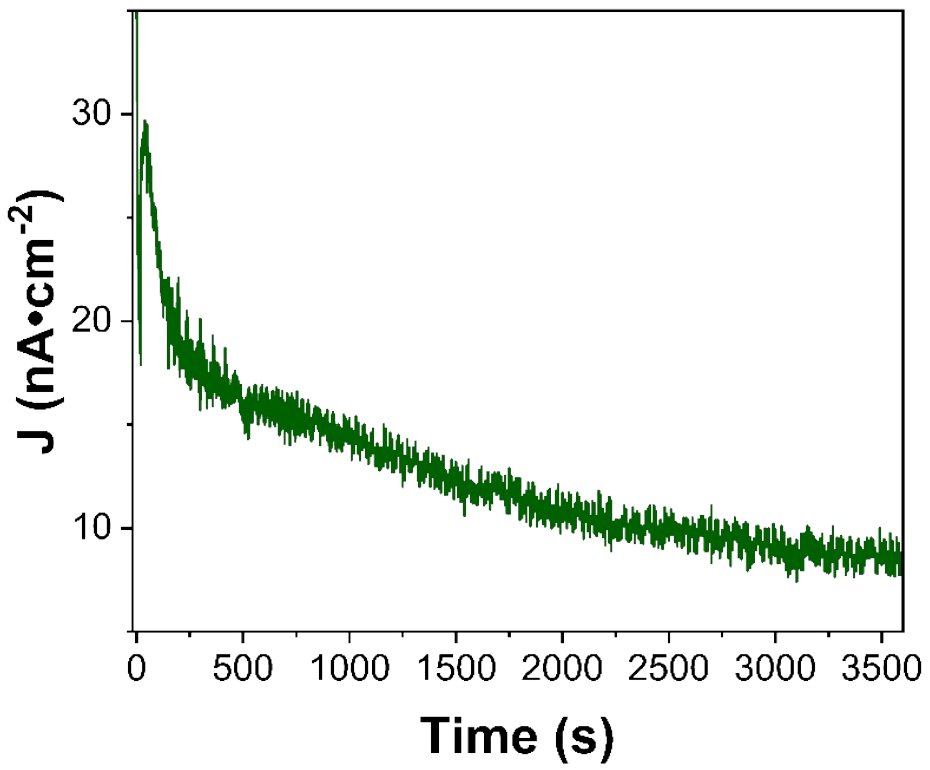

Fig.S21 Photocurrent decay test of bare PSII-based under zero bias voltage and a light power density of 70 mW•cm^{-2}.

Table S1. Photographs of CdTe QDs and PSII under illumination at 530 nm and 365

	530 nm	365 nm
CdTe QDs		
PSII		

nm

Table S2 Examples of Partially Designed Light Conversion

Materials	Photonic conversion		Application	References
	Excition (nm)	Emission (nm)		
polystyrene (PS)/ SiO_2-WO_{3-X}、Nd^{3+} 、Yb^{3+} 、Er^{3+}	808	620-700 490-570	The electrically triggered information encryption devices	8
WO_3- Yb、Er	980	525 555 600	Photocatalytic hydrogen release	9
Silicon quantum dots	488 532	432	The air stability of NC-based photon upconversion	10
Carbon dots, g-C_3N_4	355 470	420~650	Practical lighting and display applications	11
Fluorescent diarylethenes	635	532	Photofunctional materials	12
Substituted anthracene derivatives	550	400	Light emitting devices	13
WS_2	457	914	Quantum photonic systems	14
PYIT1	808	573 605	Up-conversion devices	15
Azobenzene poly (acrylic acid) ($NaYF_4$: Yb30%, Tm0.5%, Nd5%)	808	365 475	Animals imaging	16
β-NaYF4:Er^{3+}	1200	980	Photovoltaics	17

References：

1. Z. Yuan, J. Li, Y. Yang, X. Feng, J. Shen, J. Wang, L. Duan, J. Li and X. Zhang, *Colloids and Surfaces A: Physicochemical and Engineering Aspects*, 2025, **707**, 135921.
2. K. Hu, Y. Li, C. Ge, L. Bai, G. Liu, G. Qiao, S. G. Kang, E. J. Kim and M. Wang, *Sensors and Actuators B: Chemical*, 2023, **387**, 133786.
3. A. Jacob Olasoji, J. Hyuck Heo and S. Hyuk Im, *Journal of Colloid and Interface Science*, 2025, **678**, 842-853.
4. T. Lourdu Madanu, L. Chaabane, S. R. Mouchet, O. Deparis and B.-L. Su, *Journal of Colloid and Interface Science*, 2023, **647**, 233-245.
5. X. Chen, J. Xu, S. Gong, L. Zhang, N. Bi, J. Gou, Y. Li, T. Zhao and L. Jia, *Separation and Purification Technology*, 2025, **352**, 128258.
6. B. Çakıroğlu, N. Jabiyeva and M. Holzinger, *Biosensors and Bioelectronics*, 2023, **226**, 115133.
7. S. Bae, M. Kim, N. Jo, K. M. Kim, C. Lee, T.-H. Kwon, Y. S. Nam and J. Ryu, *ACS Applied Materials & Interfaces*, 2024, **16**, 16086-16095.
8. H. Xia, D. Li, J. Shang, Y. Ji, X. Yin, G. Fang, W. Xu and B. Dong, *Advanced Functional Materials*, 2023, **33**.
9. Z. Ma, X. Song, Y. Lu, F. Zhu, Y. Xie, L. Zhao, Z. Yang and J. Zhang, *Advanced Energy Materials*, 2024, DOI: 10.1002/aenm.202403307.
10. P. Xia, J. Schwan, T. W. Dugger, L. Mangolini and M. L. Tang, *Advanced Optical Materials*, 2021, **9**.
11. B. K. Barman, D. Hernández-Pinilla, O. Cretu, J. Kikkawa, K. Kimoto and T. Nagao, *Advanced Science*, 2024, **11**.
12. J. Han, J. Zhang, T. Zhao, M. Liu and P. Duan, *CCS Chemistry*, 2021, **3**, 665-674.
13. K. Börjesson, P. Rudquist, V. Gray and K. Moth-Poulsen, *Nature Communications*, 2016, **7**.
14. J. Feng, Y.-K. Wu, R. Duan, J. Wang, W. Chen, J. Qin, Z. Liu, G.-C. Guo, X.-F. Ren and C.-W. Qiu, *eLight*, 2024, **4**.
15. P. Bi, T. Zhang, Y. Guo, J. Wang, X. W. Chua, Z. Chen, W. P. Goh, C. Jiang, E. E. M. Chia, J. Hou and L. Yang, *Nature Communications*, 2024, **15**.
16. S. He, J. Song, J. Liu, L. Liu, J. Qu and Z. Cheng, *Advanced Optical Materials*, 2019, **7**.
17. G. E. Arnaoutakis, D. Busko, B. S. Richards, A. Ivaturi, J. M. Gordon and E. A. Katz, *Solar Energy Materials and Solar Cells*, 2024, **269**.